

DNA-BASED HYDROLOGICAL TRACERS: PROOF OF CONCEPT

A Thesis

Presented to the Faculty of the Graduate School

of Cornell University

In Partial Fulfillment of the Requirements for the Degree of

Master of Science

by

Asha Narayan Sharma

February 2010

© 2010 Asha Narayan Sharma

ABSTRACT

In order to answer questions that involve multiple and potentially interacting hydrological flowpaths, multiple tracers with identical transport properties that can nonetheless be distinguished from each other are required. This thesis describes the development and proof of concept of a new kind of engineered tracer system that allows a large number of individual tracers to be simultaneously distinguished from one another. This new tracer is composed of polylactic acid (PLA) microspheres into which short strands of synthetic DNA and paramagnetic iron oxide nanoparticles are incorporated. The synthetic DNA serves as the “label” or “tag” in our tracers that allow us to distinguish one tracer from another and paramagnetic iron oxide nanoparticles are included in the tracer to facilitate magnetic concentration of the tracers in water samples. The potential advantages of this strategy compared to conventional tracers are the elimination of background interferences, the ability to segregate superimposed flowpaths through the design of strictly unique DNA tags and the biodegradability of the tracers.

BIOGRAPHICAL SKETCH

Prior to joining Cornell University, Asha Sharma earned a Bachelor of Technology in Industrial Biotechnology degree from Anna University, Chennai, India. She continues in Cornell to pursue her doctorate.

Dedicated to my parents

ACKNOWLEDGMENTS

I am grateful to the many people who aided in me in the research that led to this thesis. I would like to thank Dr. Adrian Collins, Ry Forseth, John Hunt, Ruston Meyer, Inish O'Doherty , Jon Petrie, Thua Tran, and Yuanming Zhang for help and guidance at various stages. Many thanks to my committee members Drs. Todd Walter and Dan Luo, and the Cornell Soil and Water lab for constant support. I am especially grateful to Drs. Todd Walter and Michael Walter for their encouragement. If I have missed acknowledging someone, it is not due to lack of gratitude but due to my oversight, which I hope will be excused.

TABLE OF CONTENTS

Biographical Sketch	iii
Dedication	iv
Acknowledgements	v
Table of contents	vi
List of Figures	vii
List of Tables	viii
DNA-Based Hydrological Tracers: Proof of Concept	1
<i>Introduction</i>	1
<i>Materials and Methods</i>	5
<i>Results and Discussion</i>	10
<i>Conclusions</i>	17
Appendix: Fabricating Tracers	19
References	21

LIST OF FIGURES

Table 1: Results of magnetic separation experiment	13
--	----

LIST OF TABLES

Figure 1: Plot Experiment Schematic	9
Figure 2: Representative SEM image of microspheres	10
Figure 3: Distribution of microsphere size	11
Figure 4: Representative TEM image of a microsphere	11
Figure 5: Hysteresis curves	12
Figure 6: Breakthrough curve for column experiment	13
Figure 7: Result of plot experiment	15

DNA-BASED HYDROLOGICAL TRACERS: PROOF OF CONCEPT

INTRODUCTION

Tracers are used extensively in hydrology to study flowpaths, flow velocities, hydrodynamic dispersion (Flury and Wai. 2003) and other characteristics of water flow in the environment. Naturally occurring tracers such as chloride, silica, stable isotopes, and dissolved organic carbon have been used to identify contributions to streamwater from “end-members” (Christophersen and Hooper. 1992, Hooper et al. 1990) and to distinguish among contributions attributed to different hydrological processes such as runoff (Burns and Kendall. 2002), shallow subsurface flow (Brown et al. 1999), and deep groundwater (McGuire et al. 2002). Unfortunately the ubiquity of these naturally occurring chemicals makes it difficult to identify a specific flowpath, i.e. even if such a tracer identifies overland flow, it is rarely clear where the overland flow originated.

To identify flowpaths more specifically, researchers often introduce tracers that can be detected above the natural signals. A variety of traditional “artificial” or researcher-introduced tracers such as bromide (Jorgensen et al. 2004, Knopman et al. 1991), chloride (Dyck et al. 2003, Lautz et al. 2006), microspheres (Metge et al. 2007), and dyes (Flury and Wai. 2003, Heilig et al. 2003) have been used, but the applications of these are usually restricted to characterizing and/or visualizing known flowpaths at small spatial scales such as macropores (Bouma et al. 1977) , plots (Dyck et al. 2003), stream reaches (Lautz et al. 2006) because they become very dilute when applied to large scales such as watersheds. Moreover, watershed memory of past chemical inputs (Kirchner et al. 2000, Scott et al. 2001) and the sensitivity of streamwater chemical signals to interplay between biogeochemical and hydrological processes

(Hornberger et al. 2001) further complicates the use of traditional tracers. There have been several studies that use microorganisms (Harvey. 1997) and bacteriophages (Rossi et al. 1998) as tracers, however these involve limitations on size (which depends on the organism selected) and number of “labels” or “tags” available. Hydrologists have also been resourceful about using “accidental” introductions of pollutant tracers but this approach is obviously not a reliable or versatile strategy.

In order to answer questions that involve multiple and potentially interacting hydrological flowpaths, multiple tracers with identical transport properties that can nonetheless be distinguished from each other are required. A powerful, direct application of such tracers would be the identification of potential sources of so-called non-point source pollution. There are only a few examples of such tracer systems in the literature including rare earth elements (Matisoff et al. 2001, Zhang et al. 2001), fluorobenzoic acids-based systems (Benson and Bowman. 1994, Bowman and Gibbens. 1992, Dahan et al. 1999, Jaynes. 1994, Kung et al. 2000), and DNA based systems (Mahler et al. 1998, Sabir et al. 1999). The fluorobenzoic acids based system, while effective, has only a limited number (<10) of uniquely detectable tracers and is expensive (Kung et al. 2000). Moreover, their retardation and degradation rates are not identical (Bowman and Gibbens. 1992, Jaynes. 1994). The rare earth element based system is likewise hindered by a limited number of unique tracers, a.k.a. tags, and the densities of the different tags are both different from each other as well as much greater than that of water (Zhang et al. 2001). Thus, rare earth metals are really most appropriate to investigating surface water transport of sediments. For the DNA based systems, there is essentially no limitation in number of unique tracers (or tags), nor substantial differences in retardation and degradation rates. Mahler et al. (Mahler et al. 1998) attached synthetic DNA strands to silica and montmorillonite clay and measured

the DNA concentration on the particles and in the supernatant over a three week period. No further studies were done with this system. Sabir et al. (Sabir et al. 1999) used DNA not bound to any material in a 12 m forced gradient steady state field experiment. Colleuille and Kitterod (Colleuille and Kitterod. 1998) used five naked (not attached to anything) DNA “tags” along with other methods to determine the potential source of a contamination incident in a municipality production well in Norway.

We propose using biotechnology to develop an engineered tracer system that allows a large number of individual tracers to be simultaneously distinguished from one another (i.e., has a large number of potential “labels” or “tags”), can potentially be applied to watershed-scale systems (i.e., has a low detection limit) is not prohibitively expensive, is environmentally safe and will eventually degrade. This article describes our progress in developing this system, some preliminary or proof-of-concept studies, and the next steps required to make this system reliable. Specifically, we demonstrate that the tracers are fabricated as we envision, test a system for concentrating the tracers, and run two small-scale, proof-of-concept experiments.

DNA-based Microtracer Concept

Our new tracer is composed of polylactic acid (PLA) microspheres into which short strands of synthetic DNA and paramagnetic iron oxide nanoparticles are incorporated.

PLA is a polymer used here to bundle the DNA and magnetic nanoparticles into uniform and highly controllable nano- or micro-spheres. PLA is approved by the US Food and Drug Administration for medical applications and is commonly used in medical sutures and sustained release drug delivery systems (Luo et al. 1999).

Recently it has also been used in compostable food containers. One attractive property of PLA is that it tends to degrade over several weeks to months (Beck et al. 1979). The time required depends on several factors and can be somewhat controlled by manipulating the composition of the polymer via additives (Anderson and Shive. 1997). Therefore, PLA has the advantage of being biodegradable, so that it will neither pollute the environment nor hinder future experiments with its persistence, while also lasting long enough for the purposes of many hydrological investigations.

The synthetic DNA serves as the “label” or “tag” in our tracers that allow us to distinguish one tracer from another. The strands of DNA are typically about 100 bases in length. This makes their design and detection relatively simple. One advantage of using DNA as the tracer “tag” is that there are effectively limitless unique tags. Specifically, since DNA is a polymer made of four different monomers, for a strand of 100 bases, the number of unique sequences is 4^{100} or 1.61×10^{60} . Another advantage of DNA is that it allows us to use powerful biotechnology tools to “read” the tags. The Polymerase Chain Reaction (PCR) and quantitative PCR (qPCR) are highly sensitive and can detect DNA in even very dilute quantities. PCR generally indicates the presence or absence of a specific DNA sequence and qPCR allows us to quantify the number of specific DNA strands. Since the DNA strands are synthetic, that is not derived from the genome of any organism, they do not have genetic functionality. There is sometimes public concern about introducing DNA into the environment, probably due to misconceptions about biotechnology in general. People fail to recognize that DNA is ubiquitous and we all introduce copious amounts of it into the environment every day. Even so, should concerns persist, we could use segments of uncommon DNA for our tags; for example, in the Northeastern US, we could develop tags based on palm DNA since palm trees are rare in that environment.

Paramagnetic iron oxide nanoparticles are included in the tracer to facilitate magnetic concentration of the tracers in water samples. This could be important when the tracers are applied to watershed-scale systems because we anticipate that the tracers will become very dilute. Paramagnetic iron oxide particles are being studied for a range of biomedical applications including as contrast agents in MRI, in magnetic separation, in targeted drug delivery, and treatment of tumors by hypothermia (Pankhurst et al. 2003). Thus, we expect that there are low health-risks in our application of this material.

MATERIALS AND METHODS

The process for fabricating the tracers is described in the Appendix to this article.

A. Verifying Tracer Fabrication

Scanning Electron Microscopy

The external structure of the tracers was observed using a Leica Stereoscan 440 Scanning Electron Microscope (SEM). The tracers were mounted on an aluminum stub with double sided carbon tape. A Denton Vacuum Desk II sputter coater was used to coat the sample with a film of palladium/gold. The coated sample was observed under an accelerating voltage of 25 kV.

Transmission Electron Microscopy

The tracers were observed under a FEI Tecnai T-12 Transmission Electron Microscope (TEM) to ascertain incorporation of iron oxide nanoparticles. A small

drop of 1 mg/mL tracer suspension was placed on a TEM grid and allowed to air-dry before observation.

Dynamic Light Scattering

Dynamic light scattering (DLS) was used to determine the size distribution of the tracers. A small drop of 1 mg/mL sample was added to a sample vial filled with 12 mL of water. The sample was subject to dynamic light scattering on a Brookhaven Instruments BI-200 SM Research Goniometer and Laser Light Scattering System to estimate the size distribution of the microspheres.

B. Tracer Recovery and Quantification

DNA Quantification

Using DNA for our tracer tags allows us to utilize the power of qPCR to identify and quantify our tracers. To do this, the tracers were first dissolved in chloroform to release the DNA from the PLA microsphere. To 150 – 200 μ L of the sample, an equal volume of chloroform was added. The mixture was vortexed briefly and allowed to stand for 10 minutes. After 10 minutes of standing, the mixture was centrifuged. The aqueous supernatant which contained the DNA was removed using a pipette and was stored at -20 °C till QPCR was performed. QPCR was performed on a Cepheid Smart Cycler II system using the Invitrogen SYBR GreenER qPCR Master Mix and a 25 μ L total reaction volume per sample.

Magnetization Measurement

To test the efficiency of the encapsulated paramagnetic nanoparticles magnetic hysteresis curves of both the iron oxide nanoparticles and the microspheres was

measured using a vibrating sample magnetometer (VSM). Twelve 1.5 ml microcentrifuge tubes each containing 1300 μ L iron oxide suspension were centrifuged at 8500 rpm for 10 minutes. There was little or no settling. The samples were then halved in volume and 650 μ L of acetone was added to each of the 24 microcentrifuge tubes. The samples were centrifuged at 8500 rpm for 10 minutes. The supernatant (acetone containing oleic acid) was discarded. The samples were dried at 45 °C for approximately 20 minutes in the Vacufuge (Eppendorf). Samples appeared “sticky” even after drying. They were stored at 4°C for approximately 44 hours. Subsequently 300 μ L acetone was added to each of the samples. They were centrifuged at 8500 rpm for 10 minutes and the supernatant discarded. The samples were dried at 30 °C for 15 minutes in the Vacufuge. Samples appeared less sticky but appeared to have white patches, presumably of oleic acid. Unlike the iron oxide nanoparticles, the microsphere samples for magnetization measurement were not subject to any special treatment.

Magnetic Separation Experiment

Serial suspensions (concentrations ranging from 1 g/L to 0.01 mg/L) of the microspheres were made for the magnetic separation experiments; 1.5 ml of each sample was dispensed into a 1.7 ml microcentrifuge tube. The microcentrifuge tube was placed against a magnet at a location where the magnetic field was at its maximum. The magnets used were rare earth Neodymium Boron magnets sealed in Stainless Steel (Eclipse Magnetics, SR240SHS) with a maximum field of ~7600 G (measured by Alphalab, Inc. Model 1 gaussmeter) on the surface. These were kindly lent to us by Dr. Adrian Collins of ADAS, United Kingdom, Ltd. The tubes were left against the magnets overnight. With the tube still against the magnet, 1.4 ml of the “supernatant” was carefully pipetted out without touching the wall of tube closest to

the magnet. 50 μ L of water was added to the remaining water and tracers (the “concentrate”). QPCR was conducted on both the supernatant as well as the concentrate. Controls were subject to the same procedure except they were not in contact with the magnet.

C. Proof-of-Concept Experiments

For our initial tracer experiments, we chose two almost trivial systems that represent common hydrological situations. A column experiment was run to test the tracers in porous media similar to a soil or groundwater systems and a plot experiment was executed to test the tracers in an overland flow situation.

Column Experiment

A Chromaflex column from Kontes, 2.54 cm diameter and 30.5 cm tall, was filled with quartz sand of grade 12/20 (Unimin Corporation) to a height of 24.5 cm. Water was pumped to the top of the column using a Masterflex Easy-Load II LS peristaltic pump from Cole Parmer (model 77200-50) with Masterflex 06419-13 (L/S-13) tygon tubing at a flow rate of 0.111 mL/s which kept the column under saturation for the duration of the experiment. The column was first adjusted to a steady-state flow of water, and then switched to tracer solution. The concentrations of tracer solution used was 0.1 g/L . At 31.5 minutes, the input was switched back to water. Samples were collected at every 2-3 minutes, and subsequently analyzed with qPCR.

Plot Experiment

The plot experiment allowed us to scale-up our tracer application by approximately an order of magnitude relative to the column experiments (Figure 1). We chose to run the

experiments on an asphalt surface to avoid the complexities of porous media while maintaining some degree of non-idealized conditions. Approximately 400 mg of each tracer (Tags 1 and 2) dissolved in 200 ml of water were used. First a steady stream with a velocity of 0.067 m/s was established at the outlet. Tags 1 and 2 were simultaneously and instantaneously introduced 1.05 m and 2.2 m respectively from the outlet. Samples were continuously collected in 100 ml sample bottles for 269 seconds. While the attempt was made to ensure continuous sampling, some sample was lost between sample bottles. qPCR was conducted on even-numbered samples.

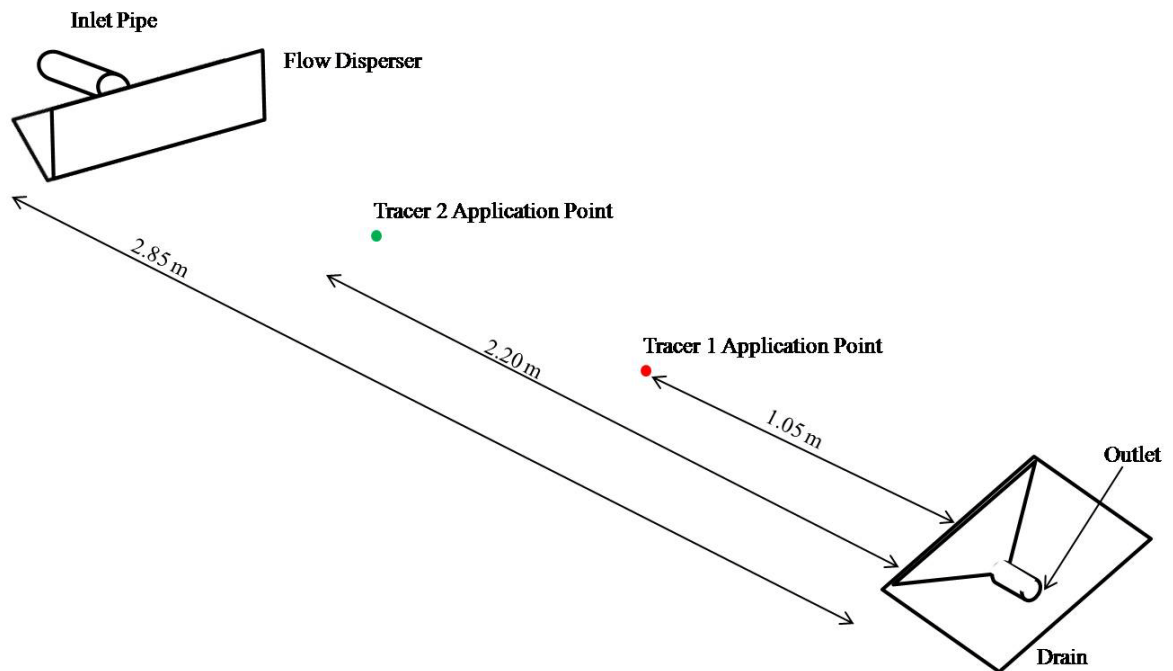


Figure 1: Plot Experiment Schematic. The tracers were applied simultaneously and instantaneously in a flow of velocity 0.067 m/s.

RESULTS AND DISCUSSION

A. Verifying Tracer Fabrication

In the SEM observations (Figure 2), the microspheres appear smooth; a range of sizes is seen, but most tracers appear to be a few hundred nm across. Figure 3 shows the results of the DLS measurements; the mean microsphere size was measured as 586.2 nm. While a narrower size distribution may be desired for future experiments, and may be obtained by other methods for making the microspheres, the available size distribution was deemed satisfactory for the preliminary experiments described here.

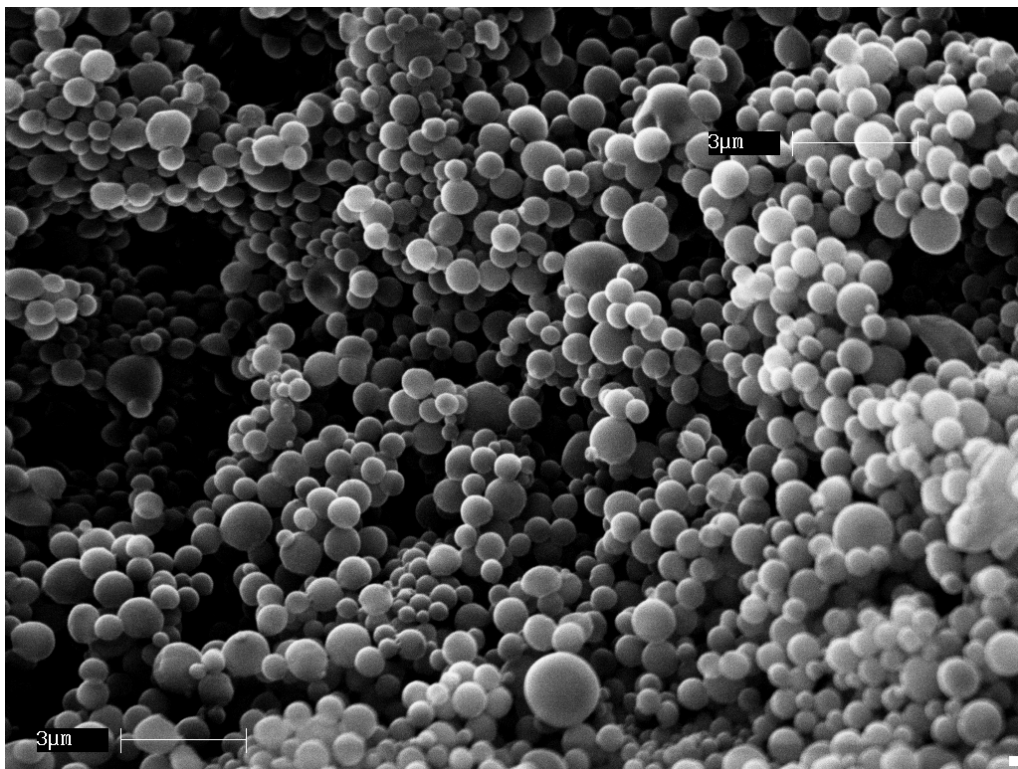


Figure 2: Representative SEM image of microspheres: the microspheres appear smooth and are mostly a few hundred nanometers in diameter.

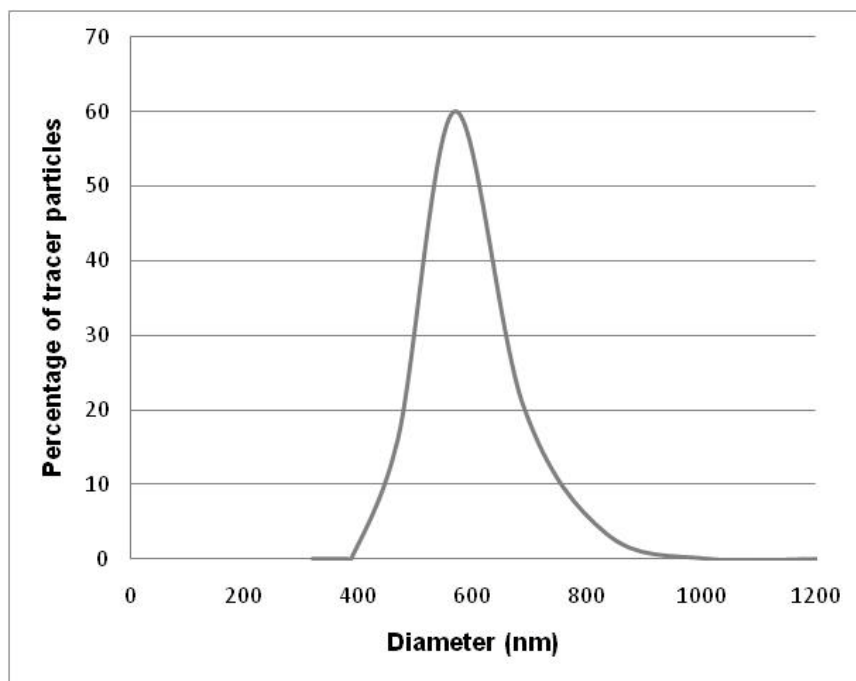


Figure 3: Distribution of microsphere size, as measured by DLS. The mean of the distribution is 586.2 nm.

TEM images revealed that the iron nanoparticles were incorporated in the microspheres (Figure 4). The magnetic hysteresis curves for the iron nanoparticles and

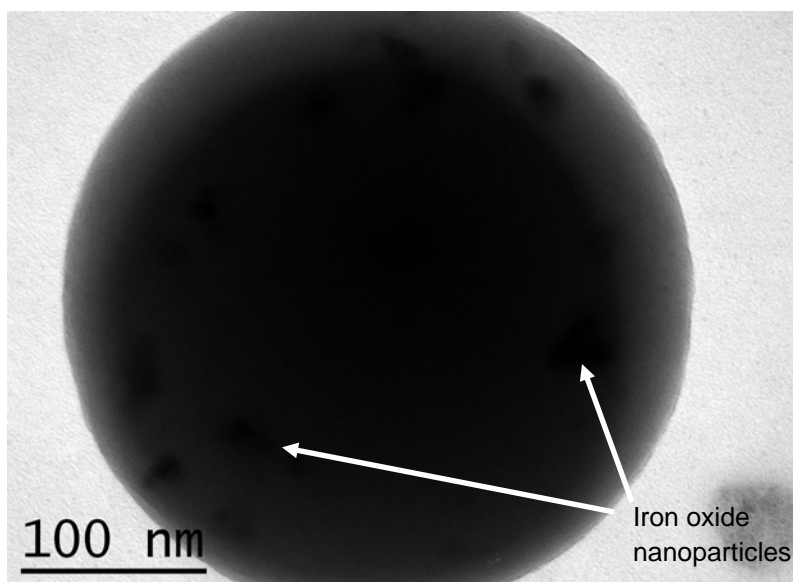


Figure 4: Representative TEM image of a microsphere: dark inclusions of iron oxide nanoparticles are seen.

microspheres are shown in Figure 5. As expected, the curves show that the

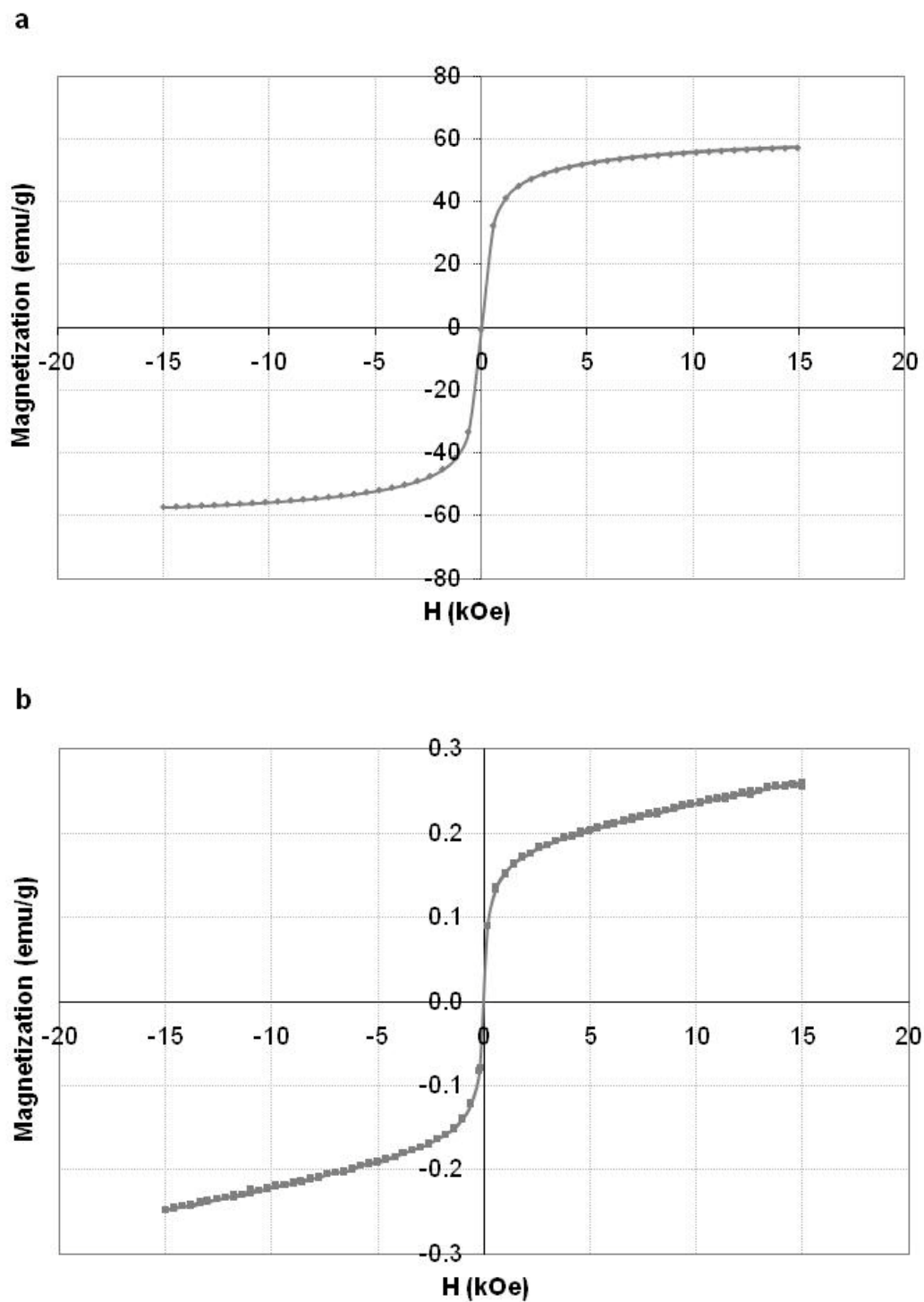


Figure 5: Hysteresis curve for (a) iron oxide nanoparticles and (b) PLA microspheres with iron oxide nanoparticles.

microspheres have no magnetization when no field is applied, but are magnetized in the presence of an external magnetic field. It is especially important that they have no magnetization in the absence of a magnetic field or they would potentially be attracted to naturally-occurring iron in the environment. For the iron oxide nanoparticles alone, the maximum magnetization was 57 emu/g. For the microspheres, the maximum magnetization was 2.6 emu/g at 15 kOe. A higher loading of iron oxide nanoparticles in the tracers would have given a higher maximum magnetization and may be explored in future, but even this level gave a good separation.

B. Tracer Recovery and Quantification

The magnetic separation experiment also verified the incorporation of the iron oxide nanoparticles in the tracers. Briefly, little or no DNA was found in the supernatant. Moreover, in the high concentration samples, the tracers were all observed to have aggregated close to the magnet while the supernatant remained clear. Unlike in the controls, there was no settling at the bottom of the tube. Table 1 shows the results of

Table 1: Results of magnetic separation experiment; the second and third columns refer to concentration of DNA in the concentrate obtained by magnetic separation and gravity separation respectively versus that in the original suspension.

Concentration (g/L)	Concentrate (magnetic separation)/Original	Concentrate (gravity separation)/Original
1	5.8	3.4
10^{-1}	5.8	2.9
10^{-2}	10.6	2.2
10^{-3}	15.0	4.5
10^{-4}	7.4	1.2
10^{-5}	7.2	2.5

the magnetic separation experiment. Magnetic separation concentrates the microspheres five- to seven-fold. While gravity for the same period of time also does concentrate the microspheres, the magnetic separation is in general at least twice as effective in concentrating the microspheres.

C. Proof-of-Concept Experiments

Column Experiment

The results of the qPCR on the samples from column experiment are shown in Figure 6. The data agree well with a simple one dimensional advection dispersion model with a dispersion coefficient of $0.39 \text{ m}^2/\text{h}$. In the case of this sand column, the tracers

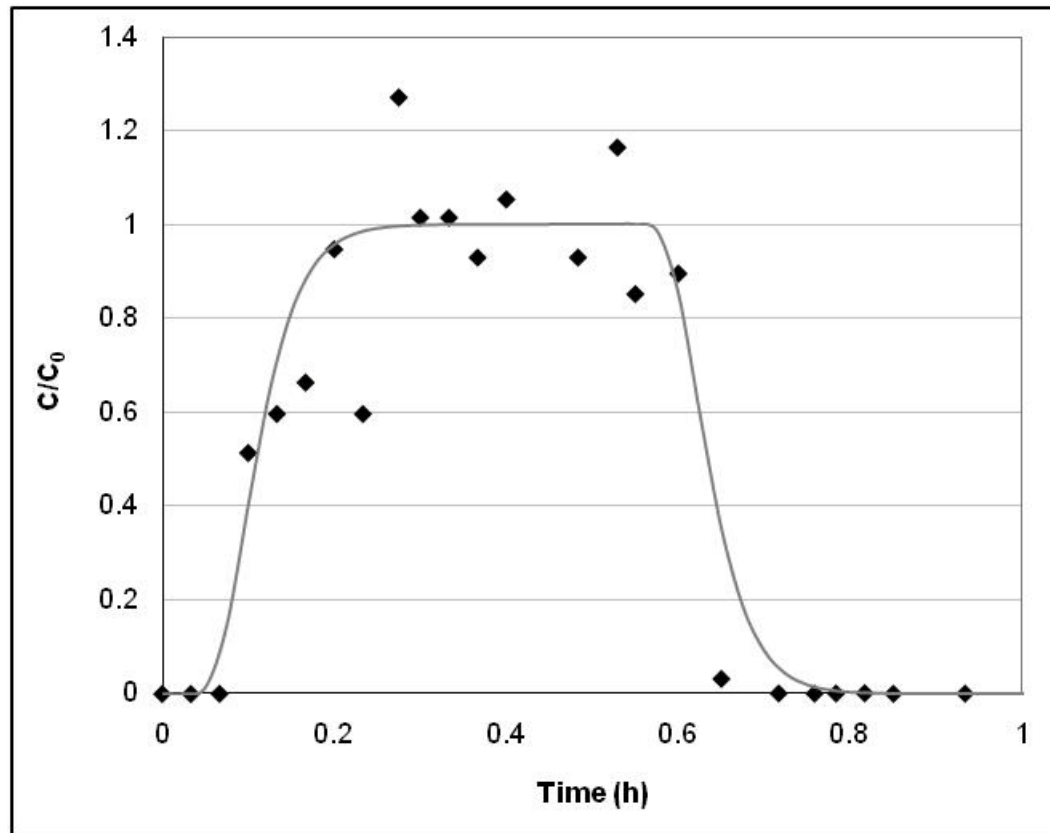


Figure 6: Breakthrough curve for column experiment. The black diamonds are data; the dark gray line represents a simple advection dispersion model for the same system, with a dispersion coefficient of $0.039 \text{ m}^2/\text{h}$.

moved at the same speed as the water. The next step is to use soil columns with regions of variable porosity and eventually of undisturbed soil to see the degree to which the tracers favor preferential flow paths. For this proof-of-concept, however, we only wanted to demonstrate that the tracers would move through porous media in a reasonably well-behaved fashion. We acknowledge that there is substantial scatter in our data, but we speculate that this can be reduced as we perfect our qPCR technique.

Plot Experiment

The results of QPCR on the samples from the plot experiment are shown in Figure 7.

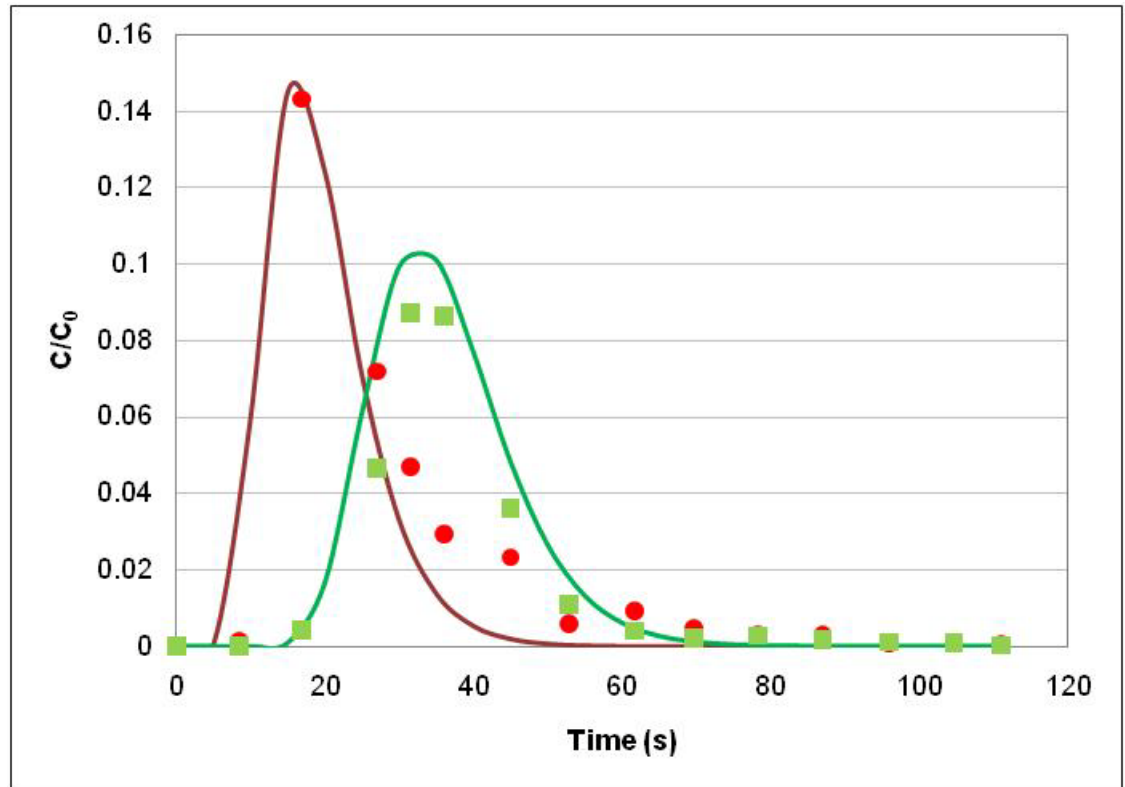


Figure 7: Result of plot experiment. Red circles are Tag 1 data; green squares are Tag 2 data; the red line represents the model for Tag 1; the green line represents the same model for Tag 2.

The data agree reasonably well with a simple one dimensional advection dispersion model with a loss factor:

$$C = \frac{1}{K} \frac{M}{2\sqrt{\pi t D}} e^{-\left(\frac{X^2}{4Dt}\right)}$$

where C is the concentration, K is a loss factor, M is the total mass introduced, t is time, D is the dispersion coefficient, and X is the distance from the center of the mass. Here D is $0.005 \text{ m}^2/\text{s}$ and K is 6.6 . The differences between the data and model can be partially explained by the fact that qPCR was not as reliable for Tag 1 as it was for Tag 2. Some error could also have been introduced due to the difficulty of taking accurate time measurements at a frequency of a few seconds.

The high K implies that there is high degree of settling of the tracers, presumably immediately after application. We speculate that this occurred because of aggregation of the tracers due to the high concentration of the input tracer suspension. Note, we added extra high quantities in this plot experiment because we were concerned about losing them in the rough surface. Originally we assumed there would be some loss of tracers as they were trapped and released from the surface similar to Shaw et al. (Shaw et al. 2009). However, the observed behavior was clearly inconsistent with a model that included a decay term. For this experimental set-up, the recovered tracers were subjected only to advection and dispersion. Furthermore, advection was at the same speed as the flowing water and dispersion was the same for both tracers. In short, we demonstrate that we can fabricate distinguishable tracers that have identical transport properties.

The next field demonstration steps are to run plot scale experiments under rainfall conditions on both impermeable (asphalt) and permeable (soil) surfaces. A small

watershed (10 ha) has been instrumented for a larger scale experiment in the near future.

CONCLUSIONS

These preliminary experiments show encouraging potential for this new tracer system. There are currently some uncertainties in the process of making the microspheres, including variability of incorporation of DNA and iron oxide nanoparticles in the tracers, and some loss at each washing step. Some iron oxide nanoparticles could additionally have been lost due to attraction to the magnetic stir bar. These processes can however be standardized to a large extent with more sophisticated equipment, resulting in more consistent microspheres with a higher load of DNA as well as iron oxide nanoparticles. We also need to find ways of scaling-up and speeding-up the process of making the tracers; the current method is somewhat labor intensive.

The magnetic separation needs to be improved for more effective concentration of the tracers. Part of this may be achieved by encapsulating more iron oxide into the tracers and part might require experimenting with different magnet-sample systems. The qPCR detection may likewise be automated and refined to improve consistency of quantification and speed of processing samples. Most of all, we think that better designs of tags and corresponding primers will lower our detection limits and make our quantification more precise.

The focus of future application studies will include running experiments with different tracer sizes, exploring transport in more complex porous media and scaling up field

experiments to more complicated conditions. The experiments described here prove the concept, and justify further experiments using this system.

APPENDIX: Fabricating Tracers

Synthetic DNA Strands

Synthetic DNA was ordered from IDT DNA (Coralville, Iowa, USA). In this study, two types of DNA strands were used. The first (Tag 1) was designed using primer sequences from Clelland et al. (Clelland et al. 1999) and the sequence in between the primers reading “AboveUs Only Sky” using the cryptographic simple substitution code from the same reference. The second (Tag 2) was designed by first generating random 200 base sequences using freely available software on the GeneDesign Random DNA generator (<http://baderlab.bme.jhu.edu/cgi-bin/gd/gdRandDNA.cgi>). The IDT DNA PrimerQuest Tool (<http://www.idtdna.com/Scitools/Applications/Primerquest/>) was then used on each of these 200 base random sequence to determine a 100 base sequence for which primers had close melting temperatures which were between 55 and 60 °C.

Paramagnetic Iron Oxide Nanoparticles

Paramagnetic iron oxide nanoparticles were made using the method described in Liu et al. (Liu et al. 2006). Briefly, 1.16 g of $\text{FeCl}_3 \cdot 6\text{H}_2\text{O}$ and 0.43 g of $\text{FeCl}_2 \cdot 4\text{H}_2\text{O}$ were dissolved in 40 ml of water under argon gas with vigorous stirring at 90 °C. 1.5 ml of 20% NH_4OH was added to the solution, followed by 0.9 ml of oleic acid which was added dropwise. Unlike in Liu et al., the solution did not separate and was used as a whole in further steps.

Microspheres

Microspheres are made using the double emulsion method commonly used for studies on sustained release drugs. Briefly, 4 ml of dichloromethane is added to approximately 200 mg of PLA to dissolve it. Nature Works PLA 3251D was a gift from Jamplast,

Inc. Once dissolved 50 uL of (nM DNA), 50 uL of the iron oxide suspension made as described above and 4 ml of 1% Polyvinyl acetate (PVA) are added. The mixture is briefly vortexed, and then homogenized for 90 seconds. The emulsion so created is added to 100 ml of 0.3 % PVA stirring at 550 rpm. After 3.5 hours of stirring, the suspension is vortexed at 4000 rpm for 15 minutes and the supernatant removed. The pellet is washed using water twice. After the second wash, the supernatant is discarded and the centrifuge tube containing the pellet is kept at -80 ° C overnight. The pellet is then lyophilized overnight. This is stored at 4 °C till further use.

REFERENCES

- Anderson JM, Shive MS. Biodegradation and biocompatibility of PLA and PLGA microspheres. *Adv.Drug Deliv.Rev.* 1997 OCT 13;28(1):5-24.
- Beck LR, Cowsar DR, Lewis DH, Gibson JW, Flowers CE. New Long-Acting Injectable Microcapsule Contraceptive System. *Obstet.Gynecol.* 1979;135(3):419-26.
- Benson CF, Bowman RS. Tri-Fluorobenzoates and Tetrafluorobenzoates as Nonreactive Tracers in Soil and Groundwater. *Soil Sci.Soc.Am.J.* 1994;58(4):1123-9.
- Bouma J, Jongerius A, Boersma O, Jager A, Schoonderbeek D. Function of Different Types of Macropores during Saturated Flow through 4 Swelling Soil Horizons. *Soil Sci.Soc.Am.J.* 1977;41(5):945-50.
- Bowman RS, Gibbens JF. Difluorobenzoates as Nonreactive Tracers in Soil and Ground-Water. *Ground Water* 1992 JAN-FEB;30(1):8-14.
- Brown VA, McDonnell JJ, Burns DA, Kendall C. The role of event water, a rapid shallow flow component, and catchment size in summer stormflow. *Journal of Hydrology* 1999;217(3-4):171-90.
- Burns DA, Kendall C. Analysis of delta15N and delta18O to differentiate NO3 - sources in runoff at two watersheds in the Catskill Mountains of New York. *Water Resour.Res.* 2002;38(5):9/1,9/12.
- Christophersen N, Hooper RP. Multivariate-Analysis of Stream Water Chemical-Data - the use of Principal Components-Analysis for the End-Member Mixing Problem. *Water Resour.Res.* 1992;28(1):99-107.

Clelland CT, Risca V, Bancroft C. Hiding messages in DNA microdots (vol 399, pg 533, 1999). *Nature* 1999 DEC 16;402(6763):750-.

Colleuille H, Kitterod NO. Forurensning av drikkevannsbrønn på Sundreoya i Al kommune. Resultat av sporstoff-forsøk. 1998;18.

Dahan O, Nativ R, Adar EM, Berkowitz B, Ronen Z. Field observation of flow in a fracture intersecting unsaturated chalk. *Water Resour.Res.* 1999;35(11):3315-26.

Dyck MF, Kachanoski RG, de Jong E. Long-term movement of a chloride tracer under transient, semi-arid conditions. *Soil Sci.Soc.Am.J.* 2003;67(2):471-7.

Flury M, Wai NN. Dyes as tracers for vadose zone hydrology. *Rev.Geophys.* 2003;41(1).

Harvey RW. Microorganisms as tracers in groundwater injection and recovery experiments: a review. *FEMS Microbiol.Rev.* 1997 JUL;20(3-4):461-72.

Heilig A, Steenhuis TS, Walter MT, Herbert SJ. Funneled flow mechanisms in layered soil: field investigations. *Journal of Hydrology* 2003 AUG 25;279(1-4):210-23.

Hooper RP, Christophersen N, Peters NE. Modeling Streamwater Chemistry as a Mixture of Soilwater End-Members - an Application to the Panola Mountain Catchment, Georgia, Usa. *Journal of Hydrology* 1990;116(1-4):321-43.

Hornberger GM, Scanlon TM, Raffensperger JP. Modelling transport of dissolved silica in a forested headwater catchment: the effect of hydrological and chemical time scales on hysteresis in the concentration-discharge relationship. *Hydrol.Process.* 2001;15(10):2029-38.

Jaynes DB. Evaluation of Fluorobenzoate Tracers in Surface Soils. Ground Water 1994 JUL-AUG;32(4):532-8.

Jorgensen PR, Helstrup T, Urup J, Seifert D. Modeling of non-reactive solute transport in fractured clayey till during variable flow rate and time. J.Contam.Hydrol. 2004;68(3-4):193-216.

Kirchner JW, Feng XH, Neal C. Fractal stream chemistry and its implications for contaminant transport in catchments. Nature 2000;403(6769):524-7.

Knopman DS, Voss CI, Garabedian SP. Sampling Design for Groundwater Solute Transport - Tests of Methods and Analysis of Cape-Cod Tracer Test Data. Water Resour.Res. 1991;27(5):925-49.

Kung KJS, Kladvko EJ, Gish TJ, Steenhuis TS, Bubenzer G, Helling CS. Quantifying preferential flow by breakthrough of sequentially applied tracers: Silt loam soil. Soil Sci.Soc.Am.J. 2000;64(4):1296-304.

Lautz LK, Siegel DI, Bauer RL. Impact of debris dams on hyporheic interaction along a semi-arid stream. Hydrol.Process. 2006;20(1):183-96.

Liu X, Kaminski MD, Guan Y, Chen H, Liu H, Rosengart AJ. Preparation and characterization of hydrophobic superparamagnetic magnetite gel. J Magn Magn Mater 2006 NOV 11;306(2):248-53.

Luo D, Woodrow-Mumford K, Belcheva N, Saltzman WM. Controlled DNA delivery systems. Pharm.Res. 1999;16(8):1300-8.

Mahler BJ, Winkler M, Bennett P, Hillis DM. DNA-labeled clay: A sensitive new method for tracing particle transport. *Geology* 1998;26(9):831-4.

Matisoff G, Ketterer ME, Wilson CG, Layman R, Whiting PJ. Transport of rare earth element-tagged soil particles in response to thunderstorm runoff. *Environ.Sci.Technol.* 2001;35(16):3356-62.

McGuire KJ, DeWalle DR, Gburek WJ. Evaluation of mean residence time in subsurface waters using oxygen-18 fluctuations during drought conditions in the mid-Appalachians. *Journal of Hydrology* 2002;261(1-4):132-49.

Metge DW, Harvey RW, Anders R, Rosenberry DO, Seymour D, Jasperse J. Use of carboxylated microspheres to assess transport potential of *Cryptosporidium parvum* oocysts at the Russian River water supply facility, Sonoma County, California. *Geomicrobiol.J.* 2007;24(3-4):231-45.

Pankhurst QA, Connolly J, Jones SK, Dobson J. Applications of magnetic nanoparticles in biomedicine. *Journal of Physics D-Applied Physics* 2003 JUL 7;36(13):R167-81.

Rossi P, Dorfliger N, Kennedy K, Muller I, Aragno M. Bacteriophages as surface and ground water tracers. *Hydrology and Earth System Sciences* 1998 MAR;2(1):101-10.

Sabir IH, Torgersen J, Haldorsen S, Alestrom P. DNA tracers with information capacity and high detection sensitivity tested in groundwater studies. *Hydrogeol.J.* 1999;7(3):264-72.

Scott CA, Walter MF, Nagle GN, Walter MT, Sierra NV, Brooks ES. Residual phosphorus in runoff from successional forest on abandoned agricultural land: 1. Biogeochemical and hydrological processes. *Biogeochemistry* 2001;55(3):293-309.

Shaw SB, Parlange JY, Lebowitz M, Walter MT. Accounting for surface roughness in a physically-based urban wash-off model. *J.Hydrol.(Amst.)* 2009;367(1/2):79-85.

Zhang XC, Friedrich JM, Nearing MA, Norton LD. Potential use of rare earth oxides as tracers for soil erosion and aggregation studies. *Soil Sci.Soc.Am.J.* 2001;65(5):1508-15.